OsteoArthritis and Cartilage (2006) **14,** 1196–1202

doi:10.1016/j.joca.2006.05.006

Osteoarthritis and Cartilage

International Cartilage Repair Society

OARSI OSTEOARTHRITIS RESEARCH SOCIETY INTERNATIONAL

Prediction of collagen orientation in articular cartilage by a collagen remodeling algorithm

W. Wilson Ph.D.†, N. J. B. Driessen†, C. C. van Donkelaar Ph.D.†* and K. Ito M.D. Sc.D.†‡
† *Department of Biomedical Engineering, Eindhoven University of Technology, P.O. Box 513, 5600 MB Eindhoven, The Netherlands*
‡ *AO Research Institute, Davos, Switzerland*

Summary

Objective: Tissue engineering is a promising method to treat damaged cartilage. So far it has not been possible to create tissue-engineered cartilage with an appropriate structural organization. It is envisaged that cartilage tissue engineering will significantly benefit from knowledge of how the collagen fiber orientation is directed by mechanical conditions. The goal of the present study is to evaluate whether a collagen remodeling algorithm based on mechanical loading can be corroborated by the collagen orientation in healthy cartilage.

Methods: According to the remodeling algorithm, collagen fibrils align with a preferred fibril direction, situated between the positive principal strain directions. The remodeling algorithm was implemented in an axisymmetric finite element model of the knee joint. Loading as a result of typical daily activities was represented in three different phases: rest, standing and gait.

Results: In the center of the tibial plateau the collagen fibrils run perpendicular to the subchondral bone. Just below the articular surface they bend over to merge with the articular surface. Halfway between the center and the periphery, the collagen fibrils bend over earlier, resulting in a thicker superficial and transitional zones. Near the periphery fibrils in the deep zone run perpendicular to the articular surface and slowly bend over to angles of −45° and +45° with the articular surface.

Conclusion: The collagen structure as predicted with the collagen remodeling algorithm corresponds very well with the collagen structure in healthy knee joints. This remodeling algorithm is therefore considered to be a valuable tool for developing loading protocols for tissue engineering of articular cartilage.

Key words: Collagen, Remodeling, Knee joint, Finite element analysis.

Introduction

Tissue engineering is a promising method to treat local cartilage damage resulting from such diseases as osteoarthritis. Successful articular cartilage replacement would be substantially enhanced if the implant had the functional load-bearing properties of the native tissue[1–6]. These properties depend primarily on the quality, content and organization of the extracellular matrix, i.e., on the proteoglycans responsible for the swelling characteristics, and the collagen network, which reinforces the tissue. It is generally believed that the matrix is optimized to fulfill the load-bearing capacities, and that its structure is determined by the very same local physical loads which it must support.

Tissue engineering activities take advantage of the knowledge that mechanical loads can stimulate cells to synthesize matrix[7,8]. With such stimuli, it is possible to create tissue-engineered cartilage with sufficient proteoglycan content, but not to obtain sufficient amounts of collagen with an appropriate structural organization[9–12]. As a result, the dynamic compressive properties and especially the tensile properties of tissue-engineered cartilage are inferior to native tissue. This is currently one of the most important limiting factors in bringing tissue-engineered constructs further toward clinical application.

To enhance the mechanical properties of *in vitro* tissue-engineered cartilage, the structural organization of the collagen network needs further attention. In the deep zone of articular cartilage the collagen fibrils are orientated in the direction perpendicular to the underlying subchondral bone. In the transitional zone they bend over to merge with the articular surface[13–15]. It is hypothesized that this particular anisotropic organization is the consequence of the mechanical conditions as experienced by the chondrocytes, which adapt their environmental extracellular matrix accordingly. However, the rules by which the spatial organization of collagen fibers is related to mechanical and chemical stimuli are poorly understood. This makes it difficult to incorporate elements in tissue engineering strategies that stimulate engineered cartilage to develop the desired anisotropic organization. Two major drawbacks to experimentally unravel the mechanical conditions that lead to tissue anisotropy are that the synthesis of collagen is a slow process, and that it is currently impossible to directly visualize formation of a collagen type II network. Hence, numerical

*Address correspondence and reprint requests to: C. C. van Donkelaar, Department of Biomedical Engineering WH 4.118, Eindhoven University of Technology, P.O. Box 513, 5600 MB Eindhoven, The Netherlands. Tel: 31-40-247-3135; Fax: 31-40-244-7355; E-mail: c.c.v.donkelaar@tue.nl
Received 23 January 2006; revision accepted 9 May 2006.

evaluation of possible regulation algorithms which relate collagen fiber orientation to mechanical conditions could enhance production of tissue-engineered cartilage with appropriate functional properties.

Driessen and colleagues[16–18] recently proposed a mathematical theory for mechanically induced collagen fiber remodeling in the aortic heart valve, where collagen type I fibers reorient along the largest principal strain direction in the tissue (as opposed to changes in collagen composition). Based on analysis of bi-axially loaded tissues, this theory was later modified such that fibers align with preferred directions that are between the principal tensile strain directions, depending on the magnitude of the principal tensile strains[19]. It was shown that the typical helical collagen architecture in blood vessels can only be explained with the latter hypothesis[19]. These findings are currently applied to enhance the mechanical properties of tissue-engineered heart valves[20].

Articular cartilage has a different function and composition, and therefore different mechanical properties than cardiovascular tissues. For example the main collagen type in articular cartilage is type II; in cardiovascular tissues type I. Apart from differences in external loading, cartilage is also loaded by internal swelling pressures. It is therefore questionable whether the collagen remodeling theory of Driessen *et al.*[19,21] also applies to cartilage. However, there are indications that collagen fibers are aligned with tensile strains in cartilage, at least at its surface. Benninghoff[13] showed a causal relationship between the patterns of split lines and tensile stresses which arise at the surface of a homogeneous, elastic body when uniformly loaded. Similar findings were later reported for the glenoid cavity of the shoulder[22].

The goal of the present study is to evaluate whether the remodeling algorithm of Driessen *et al.*[19,21] is consistent with the collagen orientations observed in native articular cartilage.

Methods

COLLAGEN REMODELING ALGORITHM

In the study of Driessen *et al.*[19,21] it is proposed that collagen fibrils align with a preferred fibril direction. These preferred fibril directions $\vec{e}_{\mathrm{p}}$ are situated between the positive principal strain directions [Fig. 1(a)], and given by

$$\vec{e}_{\mathrm{p}} = \frac{g_1\vec{e}_1 \pm g_2\vec{e}_2 \pm g_3\vec{e}_3}{\sqrt{g_1^2+g_2^2+g_3^2}} \tag{1}$$

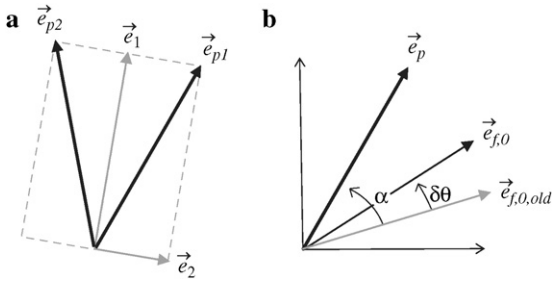

Fig. 1. (a) The preferred fibril directions $\vec{e}_{\mathrm{p}}$ are situated in between the positive principal strain directions $\vec{e}_1$ and $\vec{e}_2$. (b) The fibril direction with respect to the undeformed configuration $\vec{e}_{\mathrm{f,0,old}}$ is rotated toward the preferred fiber direction $\vec{e}_{\mathrm{p}}$ over an angle dθ to result in the new fibril direction $\vec{e}_{\mathrm{f,0}}$.

where $\vec{e}_i$ is the ith principal strain direction, and the g_i is a function of the ith principal strain (ε_i) as

$$\begin{aligned} g_i &= \varepsilon_i \quad \text{for } \varepsilon_i > 0 \\ g_i &= 0 \quad \text{for } \varepsilon_i \le 0 \end{aligned}. \tag{2}$$

Hence, only the positive principal strains ($\varepsilon_i > 0$) are used for the fibril remodeling. Note that for one positive principal strain, Eq. (1) results in only one preferred fibril direction, while for two and three positive principal strains, Eq. (1) results in two and four preferred fibril directions, respectively. The collagen fibrils reorient toward the preferred fibril directions with an angular velocity, dθ/dt,

$$\frac{\mathrm{d}\theta}{\mathrm{d}t} = \kappa\alpha = \kappa \arccos\left\| \vec{e}_{\mathrm{f,0}} \cdot \vec{e}_{\mathrm{p}} \right\|, \tag{3}$$

where α is the angle between the fibril direction in the undeformed situation $\vec{e}_{\mathrm{f,0}}$ and the preferred fibril direction $\vec{e}_{\mathrm{p}}$ [Fig. 1(b)], and κ is a positive constant that determines the rate of reorientation. The fibrils are rotated around the rotation axis

$$\vec{e}_r = \frac{\vec{e}_{\mathrm{f,0}} \otimes \vec{e}_{\mathrm{p}}}{\| \vec{e}_{\mathrm{f,0}} \otimes \vec{e}_{\mathrm{p}} \|}. \tag{4}$$

After updating the fibril direction the new strains in the tissue are computed and the new preferred fibril directions are determined. This process is repeated until homeostasis is achieved. Homeostasis is assumed when the difference between each fibril and its preferred fibril direction is less then 1° ($\alpha < 1°$). For further details about the implementation the reader is referred to Driessen *et al.*[17].

In Driessen *et al.*[19,21] $\vec{e}_i$ was determined from the left Cauchy–Green deformation tensor **B**. Hence, the fibril reorientation was first determined in the deformed state. As the fibrils were assumed to reorient with respect to the undeformed state, the fibril orientations had to be transformed back to the undeformed state. To directly asses the new fibril orientation in the undeformed state ε_i and $\vec{e}_i$ were determined from the right Cauchy–Green deformation tensor **C**. In this case the principal strain directions $\vec{e}_i$, and thereby the preferred fibril directions $\vec{e}_{\mathrm{p}}$, were defined in the undeformed state. In case of local nearly-equi-biaxial loading conditions, the two principal strain directions cannot be determined unambiguously. Hence, in these cases the fibrils were not remodeled.

MATERIAL MODEL

The deformation of articular cartilage as a result of loading is highly dependent on its time dependent behavior and internal swelling pressures. The remodeling algorithm was therefore implemented in our composition-based fibril-reinforced swelling model[23], which includes both these features. In the model articular cartilage was assumed as biphasic, consisting of a porous solid matrix saturated with water. The porous solid matrix consisted of a swelling non-fibrillar part which contains mainly proteoglycans and a fibrillar part representing the collagen network. The total tissue stress was given by[23,24]

$$\boldsymbol{\sigma}_{\mathrm{tot}} = -\mu^{\mathrm{f}}\mathbf{I} + n_{\mathrm{s,0}}\left(n_{\mathrm{coll}}\boldsymbol{\sigma}_{\mathrm{nf}} + \sum_{i=1}^{\mathrm{totf}} \rho_{\mathrm{c}}^{i}\sigma_{\mathrm{f}}^{i}\vec{e}_{\mathrm{f}}^{\,i}\vec{e}_{\mathrm{f}}^{\,i} \right) - \Delta\pi\mathbf{I}, \tag{5}$$

where μ^f is the water chemical potential, **I** the unit tensor, $\Delta\pi$ the osmotic pressure gradient, $n_{s,0}$ the initial solid volume (in the unloaded and non-swollen state), $\boldsymbol{\sigma}_{nf}$ the stress in the non-fibrillar matrix, σ_f^i the fibril stress, $\overrightarrow{e}_f^i$ the fibril direction, ρ_c^i the volume fraction of the collagen fibrils with respect to the total solid volume, n_{coll} the total collagen fraction (sum of all ρ_c^i) and i detonates the number of the fibril compartment[23,24].

Due to deformation of the tissue the fibril directions change. The new fibril directions as functions of deformation were computed as

$$\overrightarrow{e}_f = \frac{\mathbf{F}\cdot\overrightarrow{e}_{f,0}}{\left\|\mathbf{F}\cdot\overrightarrow{e}_{f,0}\right\|} \tag{6}$$

where **F** is the deformation gradient tensor and $\overrightarrow{e}_{f,0}$ the initial fibril orientation. The fibrils were assumed to be non-linear and viscoelastic. As discussed in Wilson *et al.*[25], the fibril structure was implemented as two primary and seven secondary fibril directions. As the primary fibrils represent the predominant fibril directions, and the secondary fibrils a random fibril network that stays present during life, only the primary fibrils were allowed to remodel. To determine the preferred fibril direction, α was determined for each fibril with respect to its individual preferred direction. The fibril that is closest to a preferred fibril direction is reoriented toward that preferred direction; the other fibril is reoriented toward the other preferred fibril direction.

For the non-fibrillar matrix, a compressible Neo-Hookean model was used of which the compressibility was dependent on the solid fraction[24]. As part of the water that is present in cartilaginous tissues is trapped within the collagen fibrils, the osmotic swelling pressures were based on the amount of fixed charges in the extra-fibrillar fluid[23,24,26]. All material parameters were assumed to be constant over the height of the tissue. Hence, all depth-dependent behavior in the model was the direct consequence of the composition (fluid fraction, collagen fraction, fixed charge density) and the structure (collagen orientation) of the tissue. The composition and mechanical properties used were the same as in Wilson *et al.*[23,24].

MESH AND BOUNDARY CONDITION

The remodeling law and the composition-based fibril-reinforced swelling model were implemented in an axisymmetric finite element model of the knee joint in ABAQUS v6.5 (Hibbitt, Karlsson & Sorensen, Inc., Pawtucket, RI, USA). The mesh (Fig. 2) was based on the mesh previously used in Wilson *et al.*[27]. The cartilage was loaded through a rigid impermeable flat platen. Initially there was a small gap between the indenter and the cartilage of 60 μm. The contact between the indenter and the cartilage was assumed to be frictionless. Free fluid flow was only allowed at the parts of the articular surface that were not in contact with the platen. The bottom plane was confined in all directions and the symmetry axis was confined in radial direction. In each integration point the initial fibrils' directions were orientated at $+45°$ and $-45°$ with the horizontal axis. As the model was axisymmetric, remodeling was limited to the $x-y$-plane.

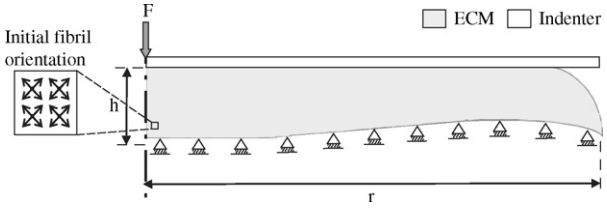

Fig. 2. Axisymmetric finite element model of a tibial plateau. The radius (r) is 16.5 mm and height (h) is 2.4 mm. The model was loaded with a force F via a rigid impermeable flat platen which is forced to remain horizontal. In each integration point the initial fibrils' directions were orientated at $+45°$ and $-45°$ with the horizontal axis.

Due to different activities during a single day, articular cartilage experiences different loads. Each of these activities results in distinct deformation of articular cartilage. Each different loading condition is bound to contribute to the final collagen orientation. Based on Morlock *et al.*[28], these loading conditions can be divided into three groups: rest, standing and walking (Table I).

During rest and stance, the joint was assumed to be loaded with a constant load and during gait with a repetitive cyclic load. Rest was assumed to take place during periods of 1×10^4 s and stance during 900 s. Based on these assumptions the loading protocol consisted of six steps:

(1) free swelling;
(2) load is ramped up to 37.5 N in 1 s (rest);
(3) load of 37.5 N is held constant for 1×10^4 s (rest);
(4) load is ramped up to 162.5 N in 1 s (stance);
(5) load of 162.5 N is held constant for 900 s (stance); and
(6) load is ramped up to 568.75 N in 1 s (gait).

As the contribution of these different activities to the final collagen structure is not known, two approaches were analyzed. In these approaches only strain-states in steps 3, 5 and 6 were taken into consideration for collagen remodeling.

(1) The averaged cartilage deformation during a day was used for remodeling of the collagen fibrils, where the preferred fibril direction was computed from the following time averaged right Cauchy–Green deformation tensor:

$$\mathbf{C}_{mean} = \sum_{j=1}^{tot\ steps}\left[\frac{n_j}{t_{tot,j}}\sum_{i=1}^{tot\ inc}\mathbf{C}_i\Delta t_i\right]. \tag{7}$$

(2) The time average of the maximal deformations during each activity was used for remodeling of the collagen fibrils, where the preferred fibril direction was computed from the following averaged right Cauchy–Green deformation tensor:

$$\mathbf{C}_{max} = \sum_{j=1}^{tot\ steps}\left(n_j\mathbf{C}_{max,j}\right). \tag{8}$$

Table I
Daily activities together with their average joint load (per knee compartment), and the time fraction this load is applied during a day (the joint loads are for a bodyweight of 65 kg)

Activity	Load (N)	Fraction of a day (n_{step})
Rest	37.5	0.73
Stance	162.5	0.19
Gait	568.75	0.08

where Δt_i is the time step of the ith increment, $\mathbf{C}_i$ the right Cauchy–Green deformation tensor of the ith increment, $\mathbf{C}_{max,step}$ the right Cauchy–Green deformation tensor that corresponds with the maximal deformation during step j, $t_{tot,j}$ the total time during step j, and n_j the weight factor for each activity (Table I).

Results

The resulting collagen orientations of the two remodeling approaches [Eqs. (7) and (8)] were almost identical (Fig. 3). There are distinct changes in collagen orientation when moving from the center of the joint toward the periphery. In the center of the tibial plateau the collagen fibrils start perpendicular to the subchondral bone and do not change orientation until just below the articular surface, where they bend over to merge with the articular surface. In this region the fibrils bend over toward both the center and the periphery of the joint. Halfway between the center and periphery the collagen fibrils start bending over earlier, resulting in thicker superficial and transitional zones. From about two-thirds of the radius of the tibial plateau the fibrils are no longer exactly perpendicular to the cement line in the deep zones. In the transition zone the fibrils preferentially bend over toward the periphery of the joint. This occurs more toward the center of the joint in the maximal averaged approach [Eq. (8)]. In the deep zone near the joint periphery, the fibrils run perpendicular to the articular surface rather than perpendicular to the subchondral bone, and slowly bend over to angles of $-45°$ and $+45°$ with the articular surface.

Discussion

This study demonstrates that the collagen remodeling algorithm of Driessen *et al.*[19,21], which was developed for collagen type I remodeling in cardiovascular tissues, can explain the collagen orientation in articular cartilage, where the loading conditions are essentially different. At the center of the joint the predicted collagen structure corresponds well with the classic arcade model of Benninghoff[13]. In this part of the joint the superficial and transitional zones are relatively thin. Together they represent approximately 12.5% of the total cartilage thickness. Toward the periphery this increases to approximately 50% of the total cartilage thickness. These findings correspond to the scanning electron microscope (SEM) measurements of Clark[14,15,29] (Fig. 4). In the studies of Clark[14,15] it was also found that the fibrils near the periphery start perpendicular to the articular surface and then directly bend over to merge with the articular surface (Fig. 4). Our model also predicts that the collagen fibrils near the periphery start perpendicular to

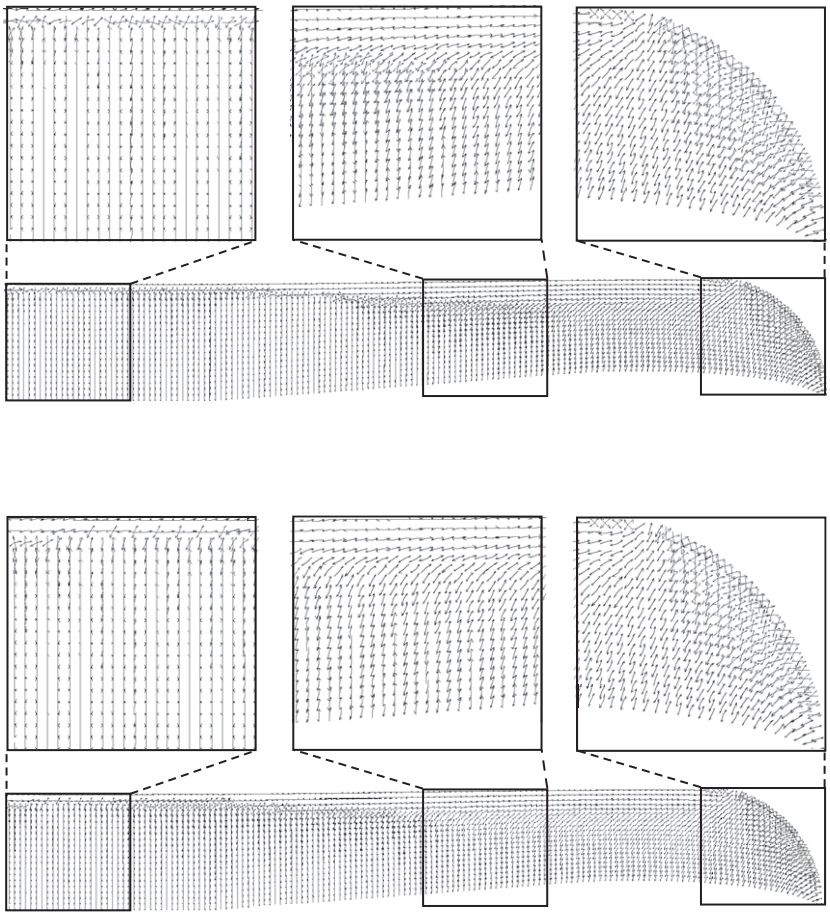

Fig. 3. Collagen structure in tibial cartilage as predicted with the collagen remodeling algorithm. Time averaged deformation (top) [Eq. (7)], time average of maximal deformation during each activity (bottom) [Eq. (8)]. The vectors represent the fibril directions in each integration point. The radius (r) is 16.5 mm and height (h) is 2.4 mm.

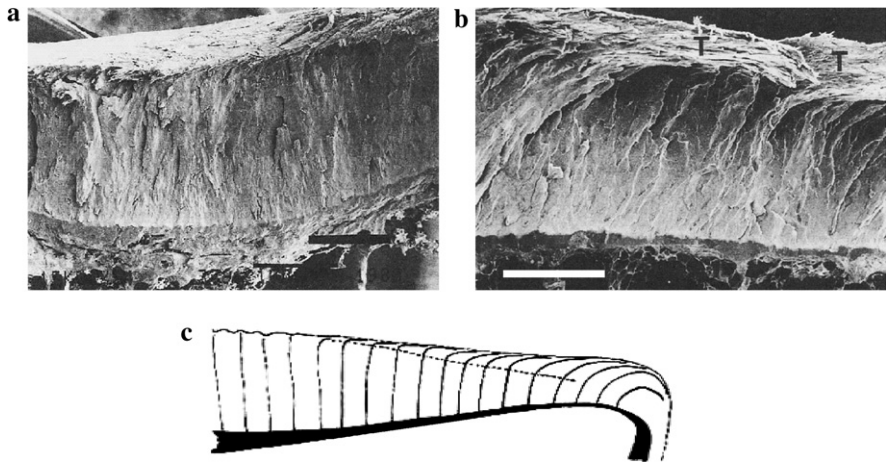

Fig. 4. Compilation of SEM data by Clark[8]. (a) SEM picture of the center of a human medial tibial plateau (bar = 1000 μm), (b) SEM picture of the periphery of a human medial tibial plateau (bar = 1000 μm), (c) schematic illustration of collagen fibril orientation across the tibial plateau (adapted from Clark[8]).

the articular surface, but bend over to angles of −45° and +45° with the articular surface. This discrepancy between model and experiment near the surface may be due to the uncertain, and therefore simplified, loading conditions that were used in this region of the model. Many authors have hypothesized that the fibrils bend over in multiple directions[13,14,30,31]. This was in agreement with the model results for center and periphery of the joint; but in between, the model predicted, the fibrils only bend over toward the periphery.

Several results of the model were unexpected. To test the robustness of the algorithm, several simulations were started with different initial collagen orientations, which all resulted in the same final structure. The simulations did not always converge to a situation in which all fibril orientations were within 1° of their corresponding preferred fibril directions in all regions. This is caused by local nearly-equi-biaxial loading conditions due to which two principal strains are equal. Although the fibrils were not remodeled in these points, this might have led to local instabilities around these points. All these instabilities occurred in the transitional zone of the cartilage, which is known to be less organized than the other zones[32–35]. In the deep zone, and in the region normally covered by the meniscus, the two primary fibril directions coincide. This indicates that there is uniaxial loading in these regions.

There are several limitations to this model, all related to applied loading conditions and geometry. First, the use of a 3D-model of the whole knee joint, including the microstructure of the articular cartilage, would have been better, but would require too much computational time. Hence, in this study an axisymmetric model was used. In the current study the subchondral bone was assumed rigid. As the subchondral bone is approximately 1000 times as stiff as the overlying cartilage, we believe the subchondral bone can be assumed rigid compared to the articular cartilage. Furthermore, as the required compositional and structural properties of the meniscus and the femoral condyle are currently not available, the tibial plateau was loaded through a rigid platen. These simplified geometric properties may explain some mismatches between the predicted structure and the findings of Clark[14,15]. Second, the loads during rest and stance were applied as static ones and the loads during gait were represented by a single ramp function. This is obviously a simplification of the actual loading conditions experienced during a day. Two averaging techniques were used to determine the average deformation of the cartilage [Eqs. (7) and (8)]. These resulted in identical final collagen configurations. This suggests that the remodeling theory is not very sensitive to the duration and the frequency of the applied loading conditions. However, it has been shown experimentally that for the production of proteoglycans and collagen dynamic loading conditions are required[36–38]. It is unknown whether dynamic loading is also required for collagen fibril orientation. For the development of a loading protocol for tissue engineering of articular cartilage a dynamic component may be necessary. Third, as the differences in composition of cartilage over the joint are not available in the literature, it was taken to be uniform. As there is a strong interaction between the local tissue composition and its mechanical behavior, in the future the addition of collagen and proteoglycan content remodeling algorithms might be beneficial. Together the simplified geometry, loading conditions and composition may have led to some inaccuracies in the predicted collagen structure. However, it's difficult to predict what the exact influence of these simplifications has been.

Despite simplifications in geometry, composition and loading conditions, the predicted collagen structure corresponds well with experimental findings. We therefore believe that, as in cardiovascular tissues, the collagen remodeling algorithm is also valid for articular cartilage. Hence, the presented remodeling theory can be a valuable tool for the development of loading protocols for tissue engineering of articular cartilage. As the numerical model is only based on composition and structure of the tissue[23,24], compositional and structural changes can directly be implemented into the model. Hence, the model can be used for samples with different compositions, and by updating the composition of the model the changes required for the loading protocol can be determined. This algorithm may also be applied to study diseases as well as treatments. During osteoarthritis the collagen structure in articular cartilage changes[39,40]. These changes are most prominent in the transitional and superficial zones[39]. The cause of these changes is currently unknown. Hence, we believe that the collagen remodeling theory as presented in this study can be a valuable tool to further improve tissue engineering of

articular cartilage, as well as understanding disease mechanisms.

To the best of our knowledge this is the first collagen remodeling theory that has been used for articular cartilage. The current remodeling model is a phenomenological one. It is currently unknown what the mechanisms for collagen remodeling in articular cartilage may be. In fibrous tissues, fibril-forming collagens are synthesized as soluble pro-collagens, which self-assemble after enzymatic cleavage. The molecules are transported in intracellular vesicles[41–43] to be discharged in deep cytoplasmic recesses that extend to the short axis of the fibroblasts, as confirmed by stacks of SEM images[44]. Since fibroblasts align with the direction of principal strain, as confirmed *in vitro* in a uni-axially loaded three-dimensional collagen lattice[45,46], it is assumed that collagen is formed in the directions of maximal strains. These fibrils can be over 2 mm long, and extend into the matrix in the direction in which the cells are aligned. A similar mechanism could modulate articular cartilage.

In conclusion, the collagen structure as predicted with the collagen remodeling algorithm corresponds very well with experimental findings. We therefore believe that, next to cardiovascular tissues, the collagen remodeling algorithm is also valid for articular cartilage. The remodeling algorithm is therefore envisaged to be a valuable tool for the development of improved loading protocols for tissue engineering of articular cartilage, and the understanding of structural adaptation in the collagen network during osteoarthritis.

Acknowledgments

This project was supported by a grant from the AO Foundation, Switzerland.

References

1. Ahsan T, Sah RL. Biomechanics of integrative cartilage repair. Osteoarthritis Cartilage 1999;7:29–40.
2. Butler DL, Goldstein SA, Guilak F. Functional tissue engineering: the role of biomechanics. J Biomech Eng 2000;122:570–5.
3. Garrett JC. Osteochondral allografts for reconstruction of articular defects of the knee. Instr Course Lect 1998;47:517–22.
4. Guilak F, Butler DL, Goldstein SA. Functional tissue engineering: the role of biomechanics in articular cartilage repair. Clin Orthop 2001;391:S295–305.
5. Morales TI, Roberts AB. Transforming growth factor beta regulates the metabolism of PGs in bovine cartilage organ cultures. J Biol Chem 1988;263:12828–31.
6. Rotter N, Aigner J, Naumann A, Planck H, Hammer C, Burmester G, *et al*. Cartilage reconstruction in head and neck surgery: comparison of resorbable polymer scaffolds for tissue engineering of human septal cartilage. J Biomed Mater Res 1998l;42:347–56.
7. Maroudas A. Biophysical chemistry of cartilaginous tissues with special reference to solute and fluid transport. Biorheology 1975;12:233–48.
8. Wong M, Carter DR. Articular cartilage functional histomorphology and mechanobiology: a research perspective. Bone 2003;33:1–13.
9. Carver SE, Heath CA. Influence of intermittent pressure, fluid flow, and mixing on the regenerative properties of articular chondrocytes. Biotechnol Bioeng 1999;65:274–81.
10. Dunkelman NS, Zimber MP, LeBaron RG, Pavelec R, Kwan M, Purchio AF. Cartilage production by rabbit articular chondrocytes on polyglycolic acid scaffolds in a closed bioreactor system. Biotechnol Bioeng 1995;46:299–305.
11. Puelacher WC, Kim SW, Vacanti JP, Schloo B, Mooney D, Vacanti CA. Tissue-engineered growth of cartilage: effect of varying the concentration of chondrocytes seeded onto synthetic polymer matrices. Int J Oral Maxillofac Surg 1994;23:49–53.
12. Waldman SD, Spiteri CG, Grynpas MD, Pilliar RM, Kandel RA. Long-term intermittent shear deformation improves the quality of cartilaginous tissue formed *in vitro*. J Orthop Res 2003;21:590–6.
13. Benninghoff A. Form und Bau der Gelenkknorpel in ihren Beziehungen zur Funktion. Z Zellforsch 1925;2: 783–862.
14. Clark JM. The organisation of collagen fibrils in the superficial zones of articular cartilage. J Anat 1990;171: 117–30.
15. Clark JM. Variation of collagen fiber alignment in a joint surface: a scanning electron microscope study of the tibial plateau in dog, rabbit, and man. J Orthop Res 1991;9:246–57.
16. Boerboom RA, Driessen NJ, Bouten CV, Huyghe JM, Baaijens FP. A finite element model of mechanically induced collagen fibre synthesis and degradation in the aortic valve. Ann Biomed Eng 2003;31: 1040–53.
17. Driessen NJ, Boerboom RA, Huyghe JM, Bouten CV, Baaijens FP. Computational analyses of mechanically induced collagen fiber remodeling in the aortic heart valve. J Biomech Eng 2003;125:549–57.
18. Driessen NJ, Peters GW, Huyghe JM, Bouten CV, Baaijens FP. Remodelling of continuously distributed collagen fibres in soft connective tissues. J Biomech 2003;36:1151–8.
19. Driessen NJ, Wilson W, Bouten CV, Baaijens FP. A computational model for collagen fibre remodelling in the arterial wall. J Theor Biol 2004;226:53–64.
20. Mol A, Driessen NJ, Rutten MC, Hoerstrup SP, Bouten CV, Baaijens FP. Tissue engineering of human heart valve leaflets: a novel bioreactor for a strain-based conditioning approach. Ann Biomed Eng 2005;33:1778–88.
21. Driessen NJ, Bouten CV, Baaijens FP. Improved prediction of the collagen fiber architecture in the aortic heart valve. J Biomech Eng 2005;127:329–36.
22. Pauwels F. Biomechanics of the Locomotor Apparatus. Berlin, Heidelberg, New York: Springer-Verlag 1980.
23. Wilson W, Huyghe JM, van Donkelaar CC. A composition-based cartilage model for the assessment of compositional changes during cartilage damage and adaptation. Osteoarthritis Cartilage. 2006 Jun;14(6): 554–60.
24. Wilson W, Huyghe JM, van Donkelaar CC. Depth-dependent compressive equilibrium properties of articular cartilage explained by its composition. Biomech Model Mechanobiol (In press).
25. Wilson W, van Donkelaar CC, van Rietbergen B, Huiskes R. A fibril-reinforced poroviscoelastic swelling (FPVES) model for articular cartilage. J Biomech 2005;38:1195–204.
26. Maroudas A, Wachtel E, Grushko G, Katz EP, Weinberg P. The effect of osmotic and mechanical pressures on water partitioning in articular cartilage. Biochim Biophys Acta 1991;1073:285–94.

27. Wilson W, van Donkelaar CC, Ito K, van Rietbergen B, Huiskes R. Pathways of load-induced cartilage damage causing cartilage degeneration in the knee after meniscectomy. J Biomech 2003;36:845–51.
28. Morlock M, Schneider E, Bluhm A, Vollmer M, Bergmann G, Müller V, *et al*. Duration and frequency of every day activities in total hip patients. J Biomech 2001;34:873–81.
29. Clark JM, Simonian PT. Scanning electron microscopy of "fibrillated" and "malacic" human articular cartilage: technical considerations. Microsc Res Tech 1997;37: 299–313.
30. Nieminen MT, Rieppo J, Toyras J, Hakumaki JM, Silvennoinen J, Hyttinen MM, *et al*. T2 relaxation reveals spatial collagen architecture in articular cartilage: a comparative quantitative MRI and polarized light microscopic study. Magn Reson Med 2001;46: 487–93.
31. Hunziker EB, Michel M, Studer D. Ultrastructure of adult human articular cartilage matrix after cryotechnical processing. Microsc Res Tech 1997;37:271–84.
32. Hasler EM, Herzog W, Wu JZ, Muller W, Wyss U. Articular cartilage biomechanics: theoretical models, material properties, and biosynthetic response. Crit Rev Biomed Eng 1999;27:415–88.
33. Mow VC, Zhu W, Ratclife A. Structure and function of articular cartilage and meniscus. In: Mow VC, Hayes WC, Eds. Basic Orthopaedic Biomechanics. New York: Raven Press, Ltd 1991:43–198.
34. Clarke IC. Articular cartilage: a review and scanning electron microscope study. 1. The interterritorial fibrillar architecture. J Bone Joint Surg Br 1971;53:732–50.
35. Broom ND, Marra DL. Ultrastructural evidence for fibril-to-fibril associations in articular cartilage and their functional implication. J Anat 1986;146:185–200.
36. Mauck RL, Soltz MA, Wang CC, Wong DD, Chao PH, Valhmu WB, *et al*. Functional tissue engineering of articular cartilage through dynamic loading of chondrocyte-seeded agarose gels. J Biomech Eng Jun 2000; 122(3):252–60.
37. Mauck RL, Seyhan SL, Ateshian GA, Hung CT. Influence of seeding density and dynamic deformational loading on the developing structure/function relationships of chondrocyte-seeded agarose hydrogels. Ann Biomed Eng 2002;30:1046–56.
38. Shelton JC, Bader DL, Lee DA. Mechanical conditioning influences the metabolic response of cell-seeded constructs. Cells Tissues Organs 2003;175: 140–50.
39. Bi X, Li G, Doty SB, Camacho NP. A novel method for determination of collagen orientation in cartilage by Fourier transform infrared imaging spectroscopy (FT-IRIS). Osteoarthritis Cartilage 2005;13:1050–8.
40. Han B, Cole AA, Shen Y, Brodie T, Williams JM. Early alterations in the collagen meshwork and lesions in the ankles are associated with spontaneous osteoarthritis in guinea-pigs. Osteoarthritis Cartilage 2002;10: 778–84.
41. Trelstad RL, Hayashi K. Tendon collagen fibrillogenesis: intracellular subassemblies and cell surface changes associated with fibril growth. Dev Biol 1979; 71:228–42.
42. Birk DE, Trelstad RL. Extracellular compartments in tendon morphogenesis: collagen fibril, bundle, and macroaggregate formation. J Cell Biol 1986;103: 231–40.
43. Birk DE, Trelstad RL. Fibroblasts create compartments in the extracellular space where collagen polymerizes into fibrils and fibrils associate into bundles. Ann N Y Acad Sci 1985;460:258–66.
44. Kadler K. Matrix loading: assembly of extracellular matrix collagen fibrils during embryogenesis. Birth Defects Res C Embryo Today 2004;72:1–11.
45. Eastwood M, McGrouther DA, Brown RA. Fibroblast responses to mechanical forces. Proc Inst Mech Eng [H] 1998;212:85–92.
46. Eastwood M, Mudera VC, McGrouther DA, Brown RA. Effect of precise mechanical loading on fibroblast populated collagen lattices: morphological changes. Cell Motil Cytoskelet 1998;40:13–21.